PHYSICS
OF NANOSTRUCTURES

Formation Mechanism of Argon Clathrates with Carbon Dendrites

M. P. Danilaev[a],*, **E. M. Zueva[b,c]**, **E. A. Bogoslov[a]**,
M. S. Pudovkin[c], and **Yu. E. Pol'skii[a]**

[a] *Tupolev Research Technical University KAI, Kazan, 420111 Russia*
[b] *Arbuzov Institute of Organic and Physical Chemistry, Kazan Scientific Center, Russian Academy of Sciences, Kazan, 420088 Russia*
[c] *Kazan Federal University, Kazan, 420008 Russia*
***e-mail: danilaev@mail.ru*
Received July 24, 2017

Abstract—The formation mechanism of argon clathrates with carbon dendrites obtained in the plasma of an atmospheric-pressure gas discharge has been studied. It has been shown that the formation of these clathrates is due to the difference between characteristic times: the lifetime of molecules surrounding argon atoms and the time of C−C bonding. It has been noted that argon clathrates with carbon dendrites can form only if a number of conditions are met: formation of molecular traps in the discharge, provision of a sufficiently low temperature at the center of the arc discharge, and the presence of active carbon particles arising from plasma decomposition of hydrocarbon precursors. Whether or not these conditions are met depends primarily on the composition of the initial hydrocarbon mixture and discharge current density, as follows from experimental data.

It is known that atoms of inert gases (Ar, Kr, Xe) may be confined in the crystal lattice of a substance the molecules of which form hydrogen bonds. Such compounds are called clathrates [1, 2]. However, a number of works [3, 4] have appeared recently where inert gas atoms were discovered in submicrometer particles of solids with an amorphous structure. Such objects are very promising for medical applications. For example, clathrates that include radioactive isotopes of inert gases and carbon or silicon submicrometer particles may be applied in radionuclide therapy of oncological diseases [5, 6]. In this field of application, precision control of radiation (hence, precision control of the number of inert gas isotopes in submicrometer particles) is required. In turn, to provide precision control of the number of inert gas isotopes in fabricating their clathrates with submicrometer particles, it is necessary to have a clear sense of their formation mechanism, which is not always obvious. After argon clathrates with carbon dendrites obtained in the arc discharge plasma were discovered, an excimer mechanism of their formation was hypothesized [3]. The aim of this work was to gain a deeper insight into the formation mechanism of inert gas clathrates with carbon dendrites.

The typical structure of a carbon dendrite obtained in the arc discharge plasma [3] is presented in Fig. 1.

In general, three regions can be distinguished in the cross section of a carbon dendrite obtaining an arc discharge (Fig. 1): (*1*) core, (*2*) intermediate layer, and (*3*) outer sheath. In each region, the dendrite structure differs in accordance with growth conditions, hydrocarbon precursors from which the dendrite forms, dis-
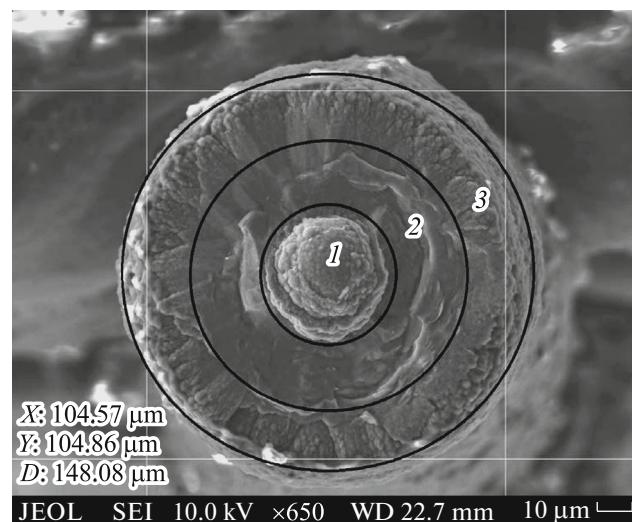

Fig. 1. Typical cross-sectional view of the carbon dendrite.

charge current density, pressure in the discharge chamber, and gas composition [3, 7]. Specifically, if the characteristic value of the kinetic temperature in the central part of the discharge is taken to be equal to 1000°C, the core consists of disordered stacks of graphene sheets. As the current density and, hence, the temperature grow, the graphene sheets become ordered and oriented radially along the temperature gradient [8]. Since graphene is impermeable to all gases [9], argon atoms may be locked in the dendrite core only if the graphene sheets are disordered. When they become ordered, argon atoms escape from the dendrite, percolating between the graphene layers.

The envisioned mechanism of argon atom trapping in the dendrite core is the generation of molecules with Ar−C bonds (trapping molecules) in the arc plasma, the characteristic lifetime of these molecules being longer than the characteristic time of C−C bonding [3]. For as long as an argon atom is confined in the molecule, graphene sheets form around it. After the decomposition of the molecule, the argon atom remains locked in the resulting cavity, since graphene sheets are disordered. However, this mechanism may take place if a number of conditions are met simultaneously: (i) the formation of molecules with Ar−C bonds in the discharge, (ii) provision of a sufficiently low temperature at the center of the arc discharge, and (iii) the presence of active carbon particles arising from plasma decomposition of initial hydrocarbons. Whether or not these conditions are fulfilled depends primarily on the composition of the initial hydrocarbon mixture and discharge current density [3, 10, 11].

To check the above mechanism, we carried out quantum-chemical computation using the MP2 and TD-CAM-B3LVP methods with the involvement of the aug-cc-pVDZ basis set and the ORCA-4.0 program package [12]. The gaseous products of polymer (polyethylene, polypropylene, polystyrene) destruction were used as hydrocarbon precursors for clathrate synthesis. They were delivered to a discharge chamber using argon as a carrier gas [13]. Since the composition of the initial hydrocarbon mixture may be crucial in the formation of argon clathrates, we estimated the energies of chemical bond homolytic decomposition in polyethylene (PE), polypropylene (PP), and polystyrene (PS). As a model for the polymeric chain, we took the $CH_3−CHR−CH_2−CH_3$ molecule, which contains the building block $−CHR−CH_2−$ of these polymers (R = H for PE, R = CH_3 for PP, and R = C_6H_5 for PS). According to MP2 calculations, the C−C and C−R bond energies are 4.2 and 4.4 eV in PE, 4.2 and 4.2 eV in PP, and 4.9 and 6.0 eV in PS. Thus, the energy needed for the homolytic decomposition of bonds is the lowest in the case of PP. It should also be noted that the resulting free radicals and the products of their recombination can produce associates with an argon atom by means of van der Waals interaction with positively polarized hydrogen atoms. However, MP2 calculations indicate that this interaction is weak (its energy is less than 0.1 eV, and the shortest Ar−H distance exceeds 3 Å) and therefore such associates are unstable.

The quantum-chemical computation showed that with PP taken as a precursor for clathrate synthesis, the initial hydrocarbon mixture delivered to the discharge mixture contains a large number of low-molecular aliphatic hydrocarbons and their radicals. This provides a high density of the discharge current. When the discharge current density is high, deep cracking with the formation of acetylene hydrocarbons and their radicals takes place.

The computer search for molecules with Ar−C bonds both on the ground-state potential energy surface (MP2) and on the excited singlet ($S = 0$), doublet ($S = 1/2$), and triplet surfaces ($S = 1$) (TD-CAM-B3LYP) was carried out. The only minimum was observed on the ground-state singlet surface, which corresponded to the HC≡C−Ar−C≡CH molecule (the Ar−C bond length is 2.14 Å). It should be noted that the existence of the F−Ar−C≡CH molecule with a shorter Ar−C bond (1.86 Å) was predicted in [14]. It was shown that the Ar−C bond in this molecule, being mostly ionic, has a small covalent component.

According to the MP2 computation, the decomposition of the HC≡C−Ar−C≡CH molecule into two HC≡C$^\cdot$ radicals and an argon atom (HC≡C−Ar−C≡CH → 2HC≡C$^\cdot$ + Ar) proceeds with energy absorption (ΔE = 1.1 eV; that is, the energy of the Ar−C bond in the HC≡C−Ar−C≡CH molecule is 0.5 eV). This transformation is notable for a high potential barrier [14]. It is more likely that the HC≡C−Ar−C≡CH molecule decomposes into an HC≡C−C≡CH molecule and an argon atom: HC≡C−Ar−C≡CH → HC≡C−C≡CH + Ar. As follows from the MP2 computation, this process goes with energy release (ΔE = −7.3 eV); that is, the HC≡C−Ar−C≡CH molecule is metastable. In addition, this process features a low potential barrier [14]; that is, the HC≡C−Ar−C≡CH molecule is prone to such a decomposition. Nevertheless, its characteristic lifetime may exceed the characteristic time of C−C bonding.

Since a high density of the discharge current may ionize an argon atom or a hydrocarbon radical, we carried out the computer search for cation molecules with Ar−C bonds. The only minimum was observed on the ground-state singlet surface, which corresponded to the HC≡C$^+$ ← Ar molecule with a very short Ar−C bond (the bond length is as small as 1.67 Å). In this molecule, the Ar−C bond is produced by the donor–acceptor mechanism (the binding energy is 3.2 eV). The HC≡C$^+$ ← Ar molecule is a trapping molecule as well: its characteristic lifetime is longer than the characteristic time of C−C bonding.

Thus, the quantum-chemical computation data indicate that argon atoms may be trapped by carbon dendrites through the formation of HC≡C−Ar−

C≡CH and HC≡C$^+$ ← Ar molecules, which are capable of confining an argon atom for a time longer than the characteristic formation time of graphene sheets. These molecules may arise when the discharge current density is high; therefore, argon atoms can be present mainly in the dendrites obtained from the products of polypropylene destruction.

To support the above conclusions, we conducted a series of experiments. The design of the experimental setup with a point-to-point steel electrode configuration in the discharge chamber was described elsewhere [10]. A discharge was initiated through an insulating barrier—1.5-mm-thick ceramic insert. The barrier discharge plasma was generated by a 25-kHz variable voltage source, and the electric field strength was varied between ~1 and 10 kV/cm accurate to ~10%. In the experiments, the condition $T_e/T \sim 10$ was provided, where T_e is the electron temperature in the barrier discharge plasma and T is the kinetic temperature near the point electrode. Carbon dendrites grew from the surfaces of the points toward each other up to closing the discharge gap.

The first series of experiments were aimed at refining the argon atom trapping in carbon dendrites. As hydrocarbon precursors for dendrite synthesis, we used the decomposition products of polymers with a benzene ring (PS) and the decomposition products of polymers without a benzene ring (PE and PP). The presence of molecules with Ar−C bonds in the gas discharge was detected by means of transmission optical spectroscopy using a StellarNet EPP2000 spectrometer with a 0.5-nm resolution. Figure 2 shows typical spectra taken at an electric field of ~10 kV/cm and discharge current density $j_{PS} \approx (25 \pm 3)$ mA/cm^2 (when the dendrites grew from the PS decomposition products), $j_{PE}/j_{PS} \approx 2$ (dendrite growth from the PE decomposition products), and $j_{PP}/j_{PS} \approx 3$ (growth from the PP decomposition products). The optical spectra depicted in Fig. 2 were normalized to the spectrum of the radiation source (DVS-25 hydrogen-discharge lamp).

The absorption spectra calculated (TD-CAM-B3LYP) for supposed trapping molecules and their decomposition products contain bands at the following wavelength (in nanometers):

434 (2), 412 (2, $f = 0.01$), 201 (1, $f = 2.96$), 199 (2), 191 (4) (HC≡C−Ar−C≡CH);

237 (1), 230 (1, $f = 0.01$), 225 (2), 194 (1), 184 (1) (HC≡C˙);

258 (2, $f = 0.01$), 188 (1), 181 (2) (HC≡C$^+$ ← Ar);

276 (1), 265 (2), 182 (2), 180 (1) (HC≡C−C≡CH); 214 (1) (HC≡C$^+$).

In calculations, the lower limit of wavelengths was 180 nm. The number of lines and oscillator strength f are parenthesized (if $f \geq 0.01$). Intense lines at wavelengths of 260 nm or below are present only in that gas discharge spectra for which the PP decomposition
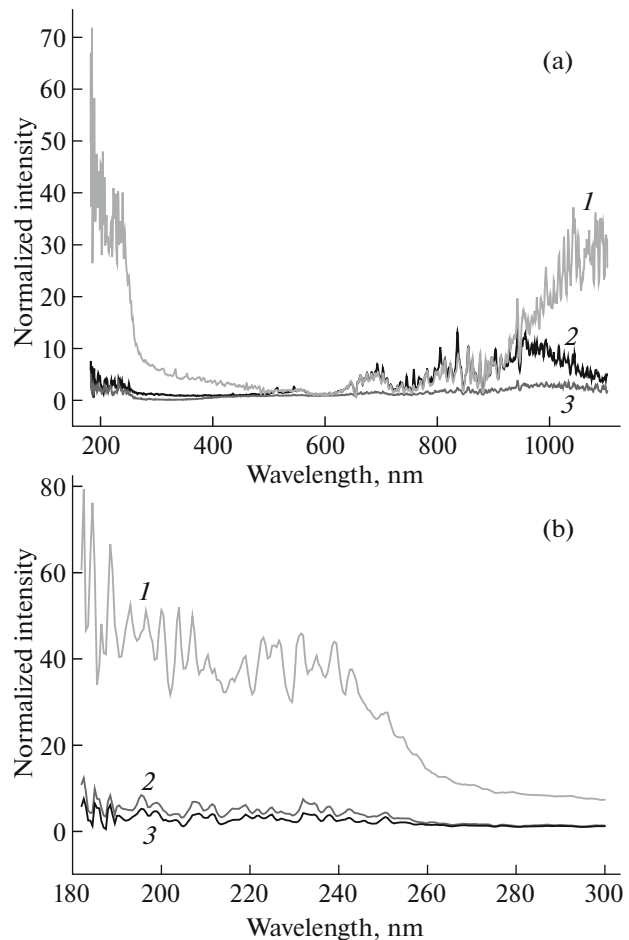

Fig. 2. (a) Normalized optical spectra of the gas discharge in which a dendrite grows from (*1*) PP, (*2*) PS, and (*3*) PE precursors and (b) the same with the short-wavelength range scaled up.

products served as hydrocarbon precursors for dendrite growth. The calculated absorption bands and the positions of the most intense lines agree well with the experimental data, indicating the fulfillment of the necessary conditions for the formation of trapping molecules in the gas discharge.

Using the method of Auger electron spectroscopy (JEOL JAMP-9510F electron spectrometer, Japan), we studied carbon dendrites to detect and locate argon atoms in them. Elemental analysis was carried out following the ASTM E 827-08 standard at a residual pressure of 10^{-9} Torr and a temperature of 23°C. Test samples were fixed to a sample holder using a conductive carbon scotch (cat. no. G3939, Agar Scientific, United Kingdom) and examined under a scanning electron microscope (SEM). The current of the primary electron beam was on the order of 10^{-8} A, and the accelerating voltage was equal to 10 kV. Points and areas for elemental analysis were selected from SEM images. Figure 3 exemplifies typical Auger spectra of dendrites obtained from the products of PS, PE, and PP decom-
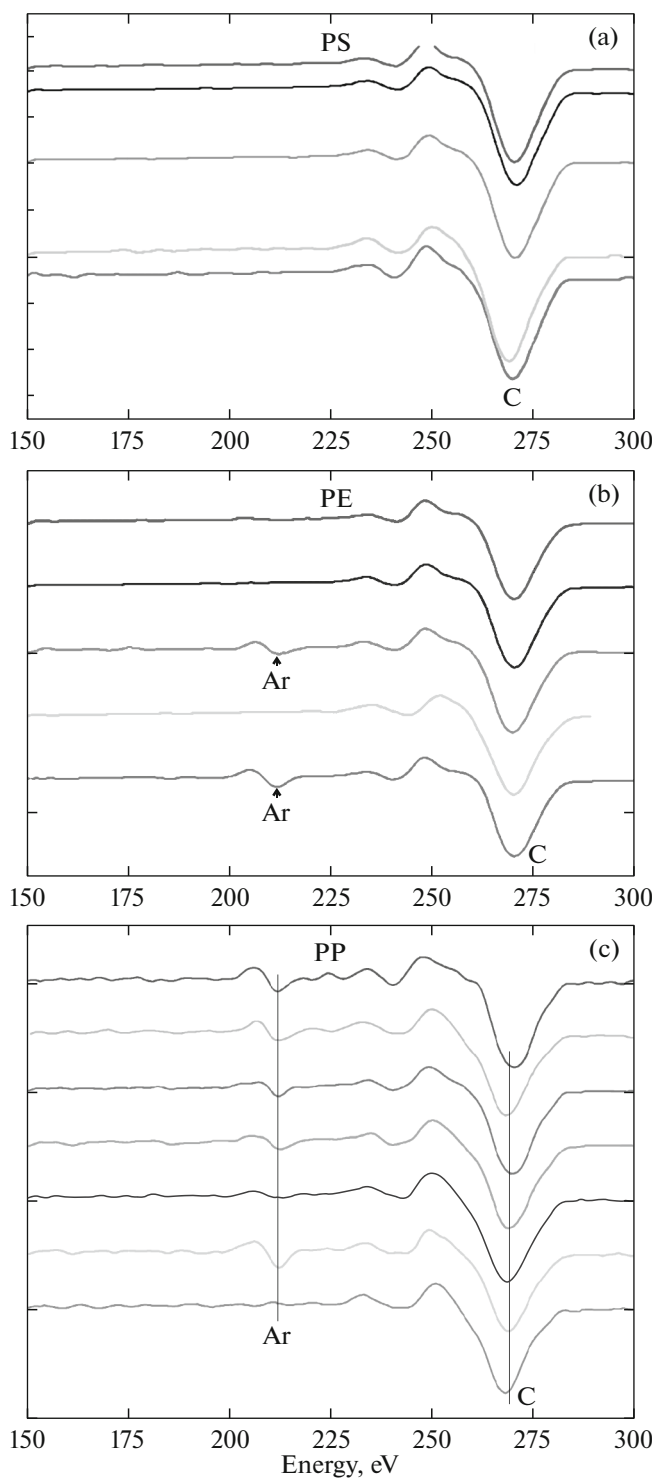
Fig. 3. Typical spectra of the dendrites grown from the products of (a) PS, (b) PE, and (c) PP decomposition.

Fig. 4. Typical spectra of the annealed dendrites.

position. The spectra were taken from the central part of several carbon dendrites synthesized under identical conditions (hydrocarbon precursors, discharge current density, field strength, and gas pressure).

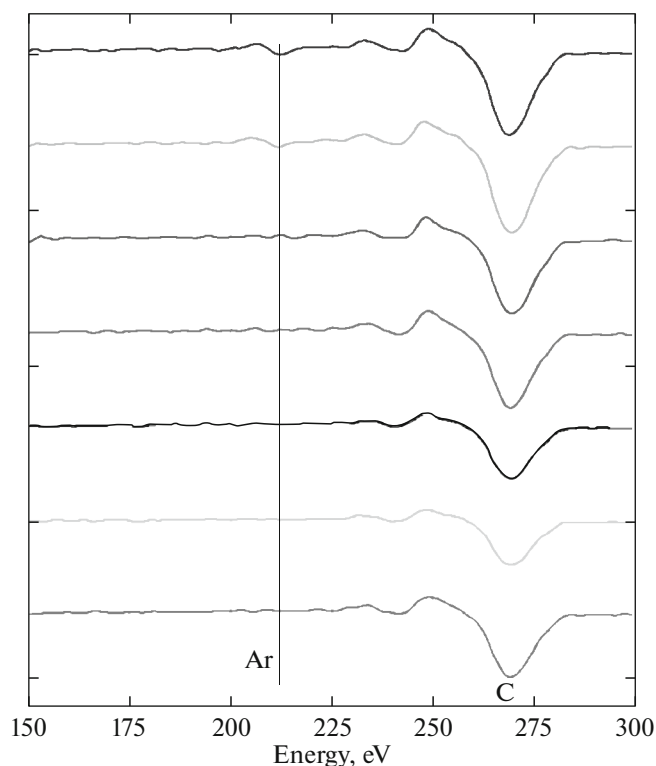Argon was found only in the central part of carbon dendrites, mostly in the dendrites obtained from the products of PP decomposition. These data correlate with the optical spectroscopy data for the gas discharge and indirectly indicate that trapping of argon atoms is associated with the formation of molecules with Ar−C bonds.

The supposition that argon atoms are confined in cavities between randomly arranged graphene sheets was checked in the second series of experiments.

Let argon atoms be actually confined in cavities between randomly arranged graphene sheets. Then, after such a carbon structure becomes ordered, the atoms will escape from these cavities. Typically, the distance between graphene layers exceeds the diameter of the argon atom [15]. Ordering of the carbon structure takes place when the temperature rises. It is worth noting that heating of randomly arranged graphene sheets in the temperature interval ~1200–2000°C causes their ordering but the structure of the sheets themselves remains unchanged [8, 15]; therefore, in the second series of experiments, carbon dendrites containing argon atoms in their core were heated to ~1500 ± 100°C at a pressure of ~$(1.0 ± 0.5) × 10^{-5}$ Torr and then these dendrites were examined again by the method of Auger spectroscopy. Typical Auger spectra of the "annealed" dendrites are presented in Fig. 4.

While the dendrites contained argon atoms before annealing, they were free of argon atoms after annealing. This confirms the supposition that argon atoms

are confined in cavities between randomly arranged graphene sheets.

Quantum-chemical calculations and experiments support the supposition that the formation of argon clathrates with carbon dendrites grown in the discharge is due to the difference between the lifetime of molecules surrounding argon atoms and the time of C−C bonding. Within the lifetime of molecules with Ar−C bonds, randomly arranged graphene sheets arise around them and the argon atoms become confined cavities between the sheets. It should be noted that argon clathrates with carbon dendrites may form only if a number of conditions are met: formation of molecular traps in the discharge, provision of a sufficiently low temperature at the center of the arc discharge, and the presence of active carbon particles arising from plasma decomposition of hydrocarbon precursors. The fulfillment of these conditions depends primarily on the composition of the initial hydrocarbon mixture and discharge current density, as confirmed by experimental data.

REFERENCES

1. A. V. Shevelkov, K. A. Kovnir, and J. V. Zaikina, in *The Physics and Chemistry of Inorganic Clathrates*, Ed. by G. S. Nolas (Springer, 2014), p. 125.

2. J. Jia, Y. Liang, T. Tsuji, S. Murata, and T. Matsuoka, Sci. Rep. **7**, 1290 (2017).

3. M. P. Danilaev, E. A. Bogoslov, Yu. E. Pol'skii, A. R. Nasybullin, M. S. Pudovkin, and A. R. Khadiev, Tech. Phys. **62**, 255 (2017).

4. D. Y. Kim and T. Kume, Jpn. J. Appl. Phys. **56**, 05FA07 (2017).

5. A. S. Thakor and S. S. Gambhir, Cancer **63**, 395 (2013).

6. T. Lammers, L. Y. Rizzo, G. Storm, and F. Kiessling, Clin. Cancer Res. **18**, 4889 (2012).

7. D. Kozak, E. Shibata, A. Iizuka, and T. Nakamura, Carbon **70**, 87 (2014).

8. G. Wang, J. Yang, J. Park, X. Gou, B. Wang, H. Liu, and J. Yao, J. Phys. Chem. C **112**, 8192 (2008).

9. D. Akinwande, C. J. Brennan, J. S. Bunch, P. Egberts, J. R. Felts, H. Gao, R. Huang, J. S. Kim, T. Li, Y. Li, K. M. Liechti, N. Lu, H. S. Park, E. J. Reed, P. Wang, et al., Extrem. Mech. Lett **13**, 42 (2017).

10. M. P. Danilaev, E. A. Bogoslov, and Yu. E. Pol'skii, Tech. Phys. Lett. **40**, 857 (2014).

11. B. M. Smirnov, Sov. Phys. Usp. **26**, 31 (1983).

12. F. Neese, Wiley Interdiscip. Rev.: Comput. Mol. Sci. **2**, 73 (2012).

13. M. P. Danilaev, E. A. Bogoslov, O. G. Morozov, A. R. Nasybullin, D. M. Pashin, and Yu. E. Pol'skii, J. Eng. Phys. Thermophys. **88**, 774 (2015).

14. A. Cohen, J. Lundell, and R. B. Gerber, J. Chem. Phys. **119**, 6415 (2003).

15. A. A. Deshmukh, S. D. Mhlanga, and N. J. Coville, Mater. Sci. Eng. R **70**, 1 (2010).

Translated by V. Isaakyan